7

Metal-Assisted Proton Transfer in Guanine-Cytosine Pair: An Approach from Quantum Chemistry

Toru Matsui, Hideaki Miyachi,
Yasuteru Shigeta and Kimihiko Hirao
Department of Applied Chemistry, School of Engineering, The University of Tokyo
Japan

1. Introduction

Since the discovery of the double helix structure by Watson and Crick, deoxyribo-nucreic acid (DNA) has been the most important substance in molecular biology. DNA consists of base, sugar and phosphoric acid. There are four kinds of base in natural DNA, adenine (A), cytosine (C), guanine (G) and thymine (T) as shown in Figure 1.

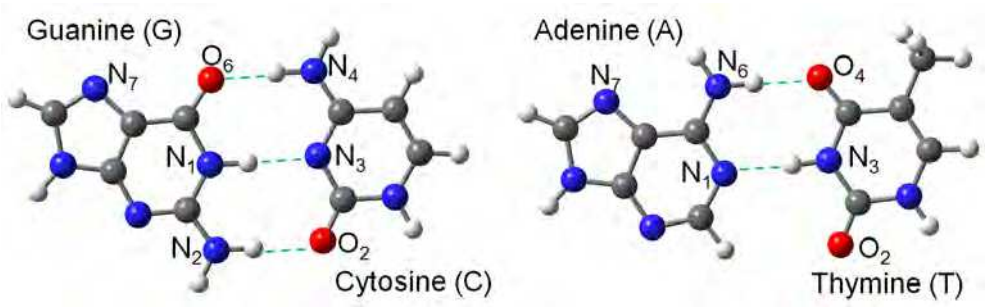

Fig. 1. The chemical structures of base pair (GC and AT pair), where the broken lines represents the hydrogen bond.

From the view of chemistry, DNA is one of the most remarkable examples for self-assembled materials existing in nature. It is said that the phosphoric acid has hydrophilic properties. This is why DNA is stable in aqueous phase. Moreover, there are two kinds of interaction which stabilizes the whole structures of DNA base pairs. These interactions are the driving force of self-assemble which leads to beautiful double helix structure. Structures of double-stranded DNA are stable in aqueous solution, because there are two kinds of interaction between Watson–Crick nucleobases. The first is the hydrogen bonding between nucleobases, where an A-T and a G-C base pairs have two and three hydrogen bonds per pair, respectively. The second is a base stacking interaction caused by π-π interaction between the base pairs. This type of interaction mainly originates from the van der Waals forces.

Hydrogen bond is important factor for interaction within DNA base pair. Many theoretical studies have computed the hydrogen bonding energy between nucleobases in a base pair. According to the most accurate computation up to date, hydrogen bonding energies of an adenine-thymine (AT) pair and a guanine-cytosine (GC) pair are about 60 and 110 kJ/mol, respectively [1, 2].

One of the most important topics in the hydrogen bonding between DNA bases is the proton-transfer (PT) reaction. In 1963, Löwdin proposed the possibility of a proton-tunneling model in the DNA base pairs [3]. He also suggested a simultaneous double proton-transfer (DPT) in AT and GC pairs, which may cause a mutation in the structure of DNA. The process of DNA mutation through proton-transfer (PT) may be estimated by computational chemistry using small molecular model systems such as several DNA base pairs. In particular, two types of the PT reaction in a GC pair (illustrated in Figure 2) have been studied extensively. One is a single proton-transfer (SPT) reaction, in which a hydrogen atom moves from N_1 of guanine (N_1 (G)) to N_3 of cytosine (N_3 (C)) as a proton. Thus, the SPT reaction causes ion pair $G\text{-}C^+$ to form, where the proton donor G becomes negative and the proton acceptor C becomes positive. The other is the DPT reaction, in which two hydrogen atoms (one hydrogen atom is located at N_1 (G)-H…N_3 (C), the other is located at O_6 (G)…H-N_4 (C)) move to the other side of each hydrogen bond, which results in G^*C^* pair (G^* and C^* represent an isomer of guanine and cytosine, respectively). In the original DNA base pair, the DPT reaction does not affect the sum of charges on each base. Unfortunately, there is very little evidence to confirm the existence of proton-transferred base pairs at room temperature by experiments, because it is difficult to determine the position of each hydrogen atom in nucleobases accurately. In this circumstance, theoretical simulations can help one to understand whether or not the PT reactions occur in DNA base pair.

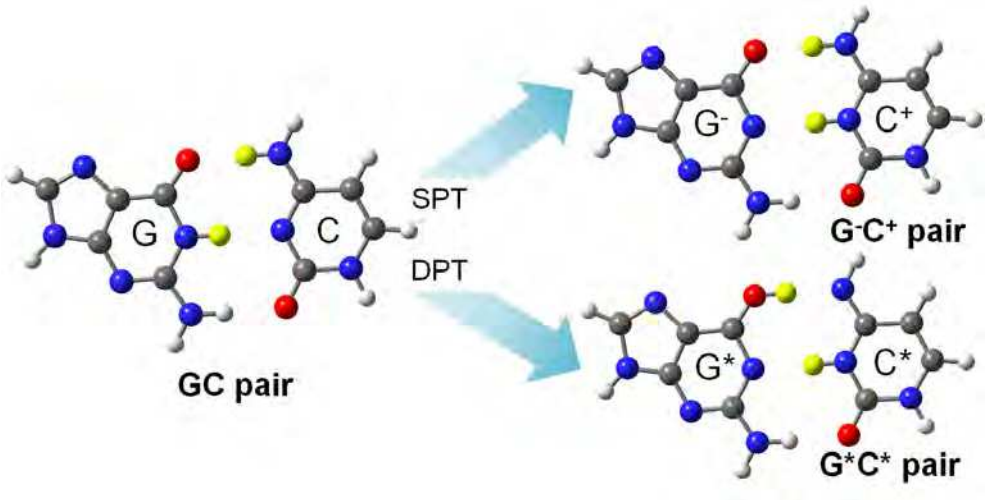

Fig. 2. Proton-transfer reaction between guanine-cytosine (GC) pair.

In order to understand the transition probability to the product or the dynamics simulation of PT reaction, we need the potential energy surface (PES) of the proton between base pair. Since the PES should be drawn within the error of chemical accuracy (1 kcal/mol= 4.2

kJ/mol), we use the quantum chemical approach to obtain the potential energy of the proton. The quantum chemical methods (e.g. Hartree-Fock (HF), post-HF theories and density functioanl theory (DFT)) are derived from the Schrödinger equation or Kohn-Sham equation. Since the introduction of the program package such as GAUSSIAN, the quantum chemical approaches have recently been a powerful tool to investigate the molecular properties which include the PES.

Many theoretical studies have investigated the PT reactions in AT and GC pairs. Florian et al. investigated the energetics of the PT reactions in GC and AT pairs [4, 5]. They reported that the GC pair was more stable than its DPT product (G*C*) by 10 kcal/mol, and the barrier height was estimated to be 14–20 kcal/mol. The DPT reaction would occur rather than the SPT reaction because the SPT reaction causes the charge separation, forming no stable product in the ground state. As an approach to the PES of proton between base pair, Villani has investigated the PES of the protons between AT and GC pair [6] and we also performed the dynamics simulation in semi-classical method [7].

However, these PT reactions can occur easily in the presence of chemical modification of nucleobases such as metal complex binding or ionization of GC pair [8]. We take a cisplatin ($[Pt(NH_3)_2Cl_2]$) bound GC pair as an example of metal complex bound DNA base pair [9, 10]. Since cisplatin was discovered by Rosenberg et al. in 1969 [11], Pt complexes have received much attention for their effects as antitumor drugs. Cisplatin distorts the structure of DNA by making a bridged structure with N_7 of guanine (G) or adenine (A). It causes a cell disorder that leads to apoptosis of the living cell. Because cisplatin contains only 11 atoms, it has been a good target for study by quantum chemistry and has been investigated from both the experimental and theoretical viewpoints. Experimentally, it is known that the bridged structure consists of 65% 1,2-d (GpG) (denoted as cis-G-Pt-G), 25% 1,2-d (ApG) (cis-G-Pt-A), and the rest is other bridged structures [12]. Nevertheless, the existence of 1,2-d (ApA) (cis-A-Pt-A) is difficult to confirm. The distorted DNAs are observed in X-ray analysis at 1.65–2.50 Å resolutions and in NMR experiments. These structures can be freely taken from the protein databank (PDB). We draw the whole structure of DNA and cisplatin bound DNA in Figure 3.

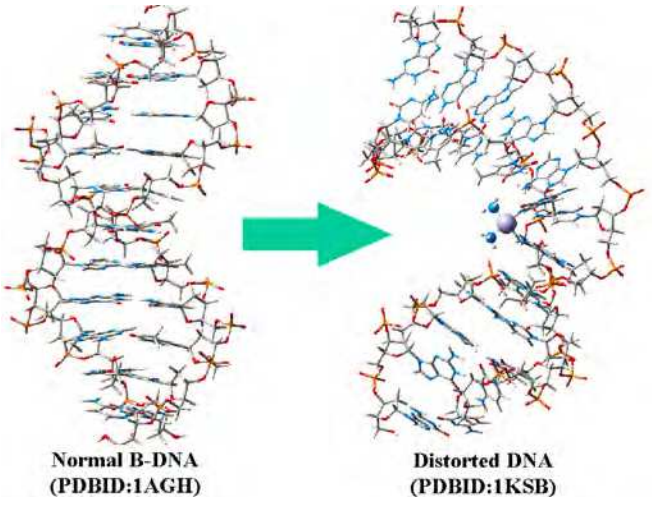

Fig. 3. Observed structure of normal DNA (B-type) and distorted structure by cisplatin.

From theoretical aspects, cisplatin has many interesting topics such as a ligand substitution, a hydration reaction, differences with transplatin and DNA binding. Ligands of cisplatin become NH_3 and/or H_2O by hydration reactions, depending on the pH of the solution. Note that the ligands of cisplatin in the human body are recognized as NH_3. In view of the DNA binding, there have been many studies of the reaction between cisplatin and DNA bases. In particular, Burda's group [13, 14] assumed [cis-Pt$(NH_3)_2$(N_7-G(or A)),(N_7-G(or A))]$^{2+}$ as the bridging structures and estimated binding energies of Pt-G and Pt-A. They found that the binding of base pair to the Pt atomtend to occur in the order of cis-G-Pt-G, cis-G-Pt-A, and cis-A-Pt-A. The angle of N_7-Pt-N_7 was about 90° for all cases. They confirmed that these bridges were stabilized by a hydrogen bond between G (or A) and a ligand of the Pt atom, such as H_2O and/or NH_3. Furthermore, reactions between cisplatin and two DNA purine bases (such as 1,2-d (GpG), 1,2-d (GpA)) were studied. Their calculated results of reaction barriers and the reaction constants of substitution reactions reproduced the experimental data well. There are two possible influences of Pt-DNA formation: (1) global structural changes, such as the distortion of the DNA duplex structure, or (2) local structural changes, such as a DNA mutation because of proton-transfer reactions. The former case is very hard to tackle with full quantum chemistry computation, because such a system is too huge study with currently available computational resource. For the latter case, the DNA mutation can be estimated using small molecular systems such as several DNA base pairs.
In this chapter, we will discuss the possibilities of simultaneous single proton transfers in one or two base pair(s). In Section 2, we will introduce a quantum chemical calculation methods, which we used on the basis of the quantum mechanics. As an application to the DNA-systems, we discuss the possibility of proton-transfer reactions in GC pair in Section 3 & 4. In Section 5, we give the concluding remarks.

2. A brief introduction to the quantum chemical calculations

In this section, we briefly explain the quantum chemical approaches used in this chapter. There are two main methods in the filed of quantum chemistry. The former is *ab initio* calculation, which is mainly used in Section 3. The latter is density functional theory (DFT), which is used in Section 4. Because of the limitation in this chapter, for the reader who wants to know the detail of the theory, we refer some textbooks for the quantum chemical approaches [15, 16].

2.1 *Ab initio* theory

The field of quantum chemistry starts from solving the Schrödinger equation for the electrons in the molecule. Because nuclei are much heavier than electrons, we can approximate that the electrons moves in the field of fixed nuclei. Then the Schrödinger equation for the electrons becomes equation (1).

$$\mathrm{H}_{\mathrm{elec}}\Psi = \left[\sum_{\mu} -\frac{1}{2}\nabla_{\mu}{}^{2} + \sum_{A}\sum_{\mu} -\frac{Z_A}{r_{A\mu}} + \sum_{\mu>\nu}\frac{1}{r_{\mu\nu}} \right]\Psi = E_{\mathrm{elec}}\Psi \,, \tag{1}$$

where A (and B in (2)), μ (and ν) represent the position of nuclei and electrons, respectively. Note here that we chose the "atomic unit" in which we set m=ħ=e=1 for simplicity. This approximation, called Born-Oppenheimer approximation, is central to quantum chemistry. The total energy E_{total} includes the repulsion between fixed nuclei, i.e.,

$$E_{total} = E_{\text{elec}} + \sum_{A>B} \frac{Z_A Z_B}{R_{AB}}. \tag{2}$$

As a wave function Ψ for the electrons, quantum chemists adopt the Slater determinant shown in (3).

$$\Psi = \sum_k c_k \Psi_k(\mathbf{x_1}, \mathbf{x_2}, \cdots, \mathbf{x_N}), \quad \Psi_k = (2\mathrm{N})!^{-1/2} \begin{vmatrix} \varphi_{k1}(\mathbf{x_1}) & \varphi_{k2}(\mathbf{x_1}) & \cdots & \varphi_{kN}(\mathbf{x_1}) \\ \varphi_{k1}(\mathbf{x_2}) & \varphi_{k2}(\mathbf{x_2}) & \cdots & \varphi_{kN}(\mathbf{x_2}) \\ \vdots & \vdots & \ddots & \vdots \\ \varphi_{k1}(\mathbf{x}_N) & \varphi_{k2}(\mathbf{x}_N) & \cdots & \varphi_{kN}(\mathbf{x}_N) \end{vmatrix}. \tag{3}$$

The variable $\mathbf{x_i}$ denotes both the coordinate **r** and its spin state (α or β). $(2N)!^{-1/2}$ is a normalization factor. This determinant satisfies the requirement called antisymmetry principle, where a sign of the wave function is changed by interchanging positions of a pair of electrons. In the quantum chemical calculation, each molecular orbital can be described as the linear combination of atomic orbitals (LCAO) $\chi_n(\mathbf{r})$ such as

$$\varphi(\mathbf{r}) = \sum_k C_k \chi_k(\mathbf{r}). \tag{4}$$

Our goal is to minimize the $E_{\text{elec}}=\langle\Psi|\mathrm{H}_{\text{elec}}|\Psi\rangle$ subject to the constraint that the trial wave function must be orthonormalized by using a variational method. This scheme is called as "Hartree-Fock(HF) theory". HF theory is categolized into the mean field theory. The working equation is given by

$$\left(-\frac{\nabla^2}{2} - \sum_A \frac{Z_A}{|\mathbf{r}-\mathbf{R}_A|} + 2\sum_{j\in\text{occ}} \int d\mathbf{r} \frac{\varphi_j^*(\mathbf{r}')\varphi_j(\mathbf{r}')}{|\mathbf{r}-\mathbf{r}'|} \right) \varphi_i(\mathbf{r}) - \sum_{j\in\text{occ}} \int d\mathbf{r} \frac{\varphi_i^*(\mathbf{r}')\varphi_j(\mathbf{r}')}{|\mathbf{r}-\mathbf{r}'|} \varphi_j(\mathbf{r}) = \varepsilon_i \varphi_i(\mathbf{r}), \tag{5}$$

where the fourth term arise from the antisymmetry principle and is referred as exhange contribution. Within the LCAO approach, above nonlinear coupled equations result in a following secular equation,

$$\mathbf{FC} = \varepsilon \mathbf{SC}, \tag{6}$$

where **F** and **S** are so-called Fock and Overlap matrices. The matrix elements are given by

$$\begin{aligned} F_{kl} &= H_{kl} + \sum_{mn} \gamma_{mn} (2V_{klmn} - V_{knml}) \\ S_{kl} &= \int d\mathbf{r} \chi_k^*(\mathbf{r}) \chi_l(\mathbf{r}) \\ H_{kl} &= \int d\mathbf{r} \chi_k^*(\mathbf{r}) \left(-\frac{\nabla^2}{2} - \sum_A \frac{Z_A}{|\mathbf{r}-\mathbf{R}_A|} \right) \chi_l(\mathbf{r}), \\ V_{klmn} &= \int\int \frac{2\chi_k^*(\mathbf{r})\chi_m^*(\mathbf{r}')\chi_l(\mathbf{r})\chi_n(\mathbf{r}')}{|\mathbf{r}-\mathbf{r}'|} \\ \gamma_{mn} &= \sum_{j\in\text{occ}} C_{mj}^* C_{nj} \end{aligned} \tag{7}$$

where H_{kl} and V_{klmn} are one- and two-electron matrix elements, respectively, and γ_{mn} is the density matrix. Since the two-electron term depends on the input density matrix, the HF equation is solved self-consistently.
HF theory covers 99.5% of the total energy of the whole molecule. However, the remaining 0.5% (equals to the order of 1-10 kcal/mol for small molecules) is quite important in the field of chemistry. To reach this accuracy, we have to consider the "electron correlation" which is the interaction between electrons. There are so many approaches (post-HF theories) to obtain the electron correlation energy. The most frequently used theory for application is the second order of Møller-Plesset (MP2) theory which is the perturbation theory for the dynamical electron correlation. This method is efficient when the HF theory gives the good results. Moreover, the computational cost is the lowest among the post-HF theories. In Section 3, we adopted this theory to obtain the PES of the proton between guanine and cytosine.

2.2 Density functional theory

The DFT is derived from the Hohenberg-Kohn theorem, which consists of two theorems: (1) The ground state electron density $\rho_0(\mathbf{r})$ of a many electron system in the presence of an external potential uniquely determines the external potential. (2) The functional $E[\rho]$ for the ground state energy is minimized by the ground state electron density ρ_0, i.e. $E[\rho_0] \leq E[\rho]$ for every trial electron density ρ. When we determine $\varphi_i(\mathbf{r})$ as a molecular orbital, as we derived the HF equation in previous paragraph, the total electron density can be determined as

$$\rho(\mathbf{r}) = \sum_{i}^{N_{occ}} |\varphi_i(\mathbf{r})|^2 . \tag{8}$$

This summation for variable i runs to the number of occupied molecular orbitals N_{occ}. Kohn-Sham equation can be written as follows:

$$\left(-\frac{\nabla^2}{2} - \sum_A \frac{Z_A}{|\mathbf{r} - \mathbf{R}_A|} + V_{\mathrm{H}}(\mathbf{r}) + v_{\mathrm{xc}}(\mathbf{r}) \right) \varphi_i(\mathbf{r}) = \varepsilon_i \varphi_i(\mathbf{r}) , \tag{9}$$

where V_H is the Hartree potential which expresses the Coulomb interaction between two electrons. The term $v_{XC}[\rho]$ is "exchange-correlation" potential which replaces the effect from the exchange of electrons used in the HF & post-HF theories. Since the equation (9) is similar to the equation (5), DFT can be used by the same procedure, i.e. LCAO approxach, as the HF theory. Although DFT includes the electron correlation effects through the empirical correlation potential, the computational cost is much lower than post HF methods. However, no one knows the exact formulation for the correlation potential so far. To obtain the exchange-correlation energy, many types of model exchange-correlation functional have been proposed. Among them, Becke proposed the exchange-correlation functional which includes the HF exchange energy. This method is often called "hybrid functional". In Section 4, we used "mPW1PW91", one of the hybrid functionals. The detailed expressions are given in ref 17.

2.3 ONIOM method

The computational cost of *ab inito* or DFT is over $O(N^3)$ where N denotes the number of atoms. Therefore, it is necessary to reduce the computational cost for larger sized molecules which is discussed in this chapter.

ONIOM, which is the abbreviation of "our own *n*-layered integrated molecular orbital and molecular mechanics" proposed by Morokuma et al. [18], is one of the candidates for the approximate ways of this problem. ONIOM is a kind of the hybrid methods for quantum mechanics/molecular mechanics (QM/MM) calculation, which is *de facto standard* of biophysical simulations. This method divides the whole molecule into two (or more) parts in order to enable us to compute different level of theories, i.e.,

$$E_{\mathrm{ONIOM}} = E_{\mathrm{low}}^{\mathrm{large}} - E_{\mathrm{low}}^{\mathrm{small}} + E_{\mathrm{high}}^{\mathrm{small}} . \tag{10}$$

When we choose the QM (*ab initio* or DFT) as the higher level calculation and molecular mechanics (MM) as the lower level, we can perform the QM/MM like calculations with this method. In the ONIOM calculation, we replace the boundary atom with a hydrogen atoms. Figure 4 shows the simple scheme for ONIOM calculations. The potential function of MM E_{MM} are generally written as follows:

$$\begin{aligned} E_{\mathrm{MM}} = & \sum_{bonds} K_r (r - r_{eq})^2 + \sum_{angles} K_\theta (\theta - \theta_{eq})^2 + \sum_{dihedrals} \frac{V_n}{2}[1 + \cos(n\varphi - \gamma)] \\ & + \sum_{i<j} [\frac{A_{ij}}{r_{ij}^{12}} + \frac{B_{ij}}{r_{ij}^{6}} + \frac{q_i q_j}{\varepsilon r_{ij}}] \end{aligned} . \tag{11}$$

These terms are the stretch (bonds), bend (bond angles), torsional (dihedral angles) and non-bonded interactions (van der Waals interaction and Coulomb interaction). The constants r_{eq}, θ_{eq}, γ are obtained by geometry optimization with quantum chemical calculation. We also have to determine the parameter K_{r}, K_θ, V_{n}, A_{ij}, B_{ij}. The variable q_{i} is called as "MM charge" which depends on the computational models. We used this scheme in Section 4.

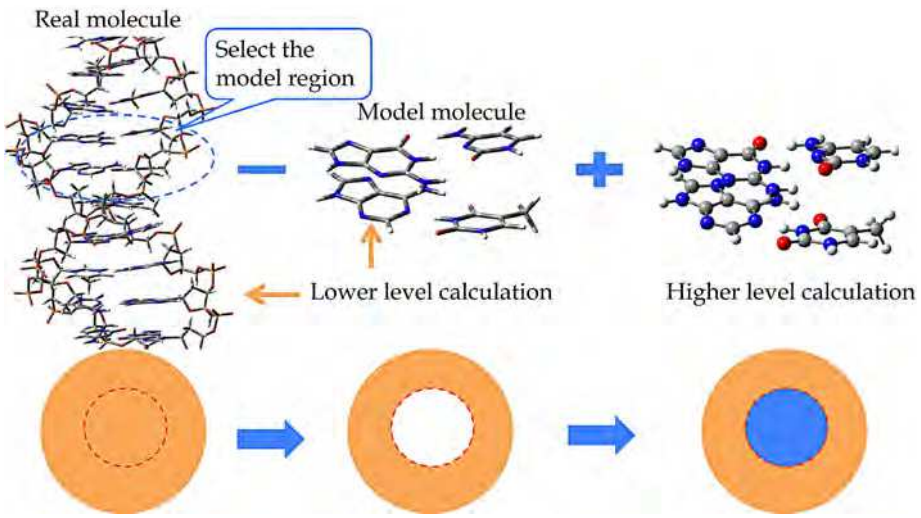

Fig. 4. An image of ONIOM scheme. In general, the region in orange is computed by the lower level theory such as molecular mechanics (MM). The region in blue is for higher level theory such as *ab initio* or DFT.

3. Local change in a cisplatin bound GC pair

3.1 Computational details

Firstly, we focused on the proton-transfer reaction between a GC pair. We simplified the model to the system which consists of one GC pair and cisplatin, i.e. $[Pt(NH_3)_3GC]^{2+}$. Geometry optimizations were first performed by the MP2 method. As the platinum is a heavy element, we have to consider the relativistic effect. In order to reduce the computational cost, we adopted an effective core potential (ECP) which implicitly includes the relativistic effect. As a typical ECP, we used the LanL2DZ basis function (We here denote this set of calculation as "MP2/LanL2DZ"). Later hydrogen bonding energy was calculated at those optimized structures with correction of a basis set superposition by the counterpoise method. All calculations were performed by GAUSSIAN03 [19]. The hydrogen bond lengths, energies, induced charges and all possible proton transfer reactions among the bases were calculated.

3.2 Local changes of properties in platinum complex bound GC pair

In this subsection, we compared neutral GC pair with the platinum complex bound GC pair. Especially, we focused on the hydrogen bonding energy, hydrogen bonding length and IR spectra. First, we summarized the results of the optimization in Table 1.

	Hydrogen bonding energy	Hydrogen bonding length [in Å]		
	[kcal/mol]	O_6(G)-N_4(C)	N_1(G)-N_3(C)	N_2(G)-O_2(C)
GC pair	27.2	2.98	2.93	2.85
Pt + GC	31.4	3.06	2.91	2.90

Table 1. Summary of the change caused by the coordination of platinum complex.

Hydrogen bond length and energy: The major difference between normal GC pair and platinum complex bound GC pair is the length between O_6(G) and N_4(C). This is caused by Pt^{2+} cation which attracts the O_6(G). As a result, the hydrogen bond length O_6(G)-N_4(C) becomes larger. On the other hand, the hydrogen bond length N_1(G)-N_3(C) is not affected by the platinum complex binding. The hydrogen bond energy of the base pairs is given by the energy difference between $[Pt(NH_3)_3G]^{2+}$ + C and $[Pt(NH_3)_3GC]^{2+}$. The results show that the hydrogen bond energy increases by 4 kcal/mol by Pt complex formation.

Changes in IR spectra: Next, the vibrational analyses were performed by MP2/LanL2DZ at the optimized structure obtained by the same method. The GC pair has three peaks of N-H stretching modes related to the hydrogen bonds. We defined three N-H stretching modes O_6…H-N_4, N_1-H…N_3 and N_2-H…O_2 as stretch1, stretch 2 and stretch 3, respectively.

Figure 5 shows the results of peak shifts before and after the Pt binding. In the case of N-H stretch between O_6 (G)-N_4 (C), about 250 cm^{-1} blue shift was observed and the intensity became lower. This means the hydrogen bonding becomes distant and weaker. In the case of N-H stretch between N_2 (G)-O_2 (C), on the other hand, about 300 cm^{-1} red shift was observed and the intensity became higher showing that the hydrogen bonding becomes stronger. These shifts can be explained by the hydrogen bonding length. In the case of N-H stretch between N_1 (G)-N_3 (C), about 400 cm^{-1} red shift was observed. From these results, it was found that the additional hydrogen bond between the H atom of the ligand and O_6 of G affects the stability of the complex.

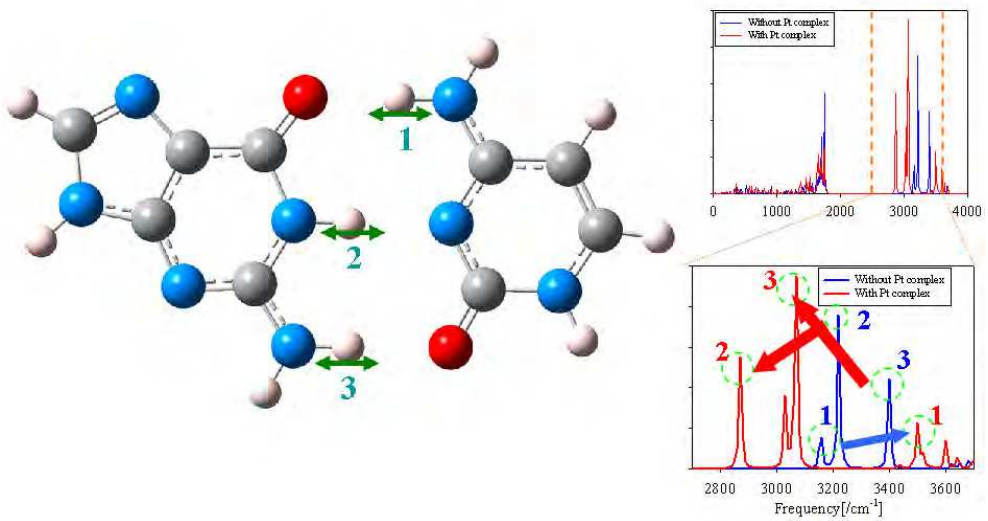

Fig. 5. IR spectra of GC pair and platinum complex bound GC pair. The peak numbers correspond to the N-H stretching modes.

3.3 Potential energy surface of proton

The other hydrogen bonds become closer because of the electrostatic interaction induced by the Pt binding. Especially, N_1 (G) and N_3 (C) become closer and the potential energy curve of the hydrogen atom between them has a double minimum. Next we proceed to investigate a feature of local changes at the hydrogen bonds by observing the PES as a function of positions of H atoms in order to understand the peak shifts. The GC pair has three hydrogen bonds: O_6…H-N_4, N_1-H…N_3 and N_2-H…O_2, respectively. We focused on the two protons: O_6…H-N_4 and N_1-H…N_3, which were concerned with the SPT or DPT reactions as shown in the introduction. We obtained an energy of optimized geometry $V(x,y)$ as a function of bond length O_6-H (x) and N_1-H (y). We fitted the PES as the following equation.

$$V(x,y)= \sum_{\substack{i,j \\ i+j\le 6}} C_{ij} x^i y^j \ , \tag{12}$$

where C_{ij} is the expansion coefficient. We used the PES of normal GC pair computed by Villani [6]. We draw the PESs as shown in Figure 6 and listed the expansion coefficients in Table 2. There are explicit differences in PESs after the Pt binding. In the normal GC pair, two local minima were found, which correspond to the DPT reaction. On the other hand, O_6-H are fixed near the global minimum, N_1-H has two minima in the platinum complex bound GC pair. The former is near N_1-H=1.10 and the latter is near N_1-H=1.70, respectively, which corresponds to SPT reaction. It was confirmed that its energy difference and energy barrier are very small.

3.4 Proton-transfer reaction in Pt+GC pair

We show the existence of the structure that undergoes SPT reaction between N_1 (G) and N_3 (C), which is hereafter denoted as a G-C^+ pair. The barrier of the DPT reaction, which occurs

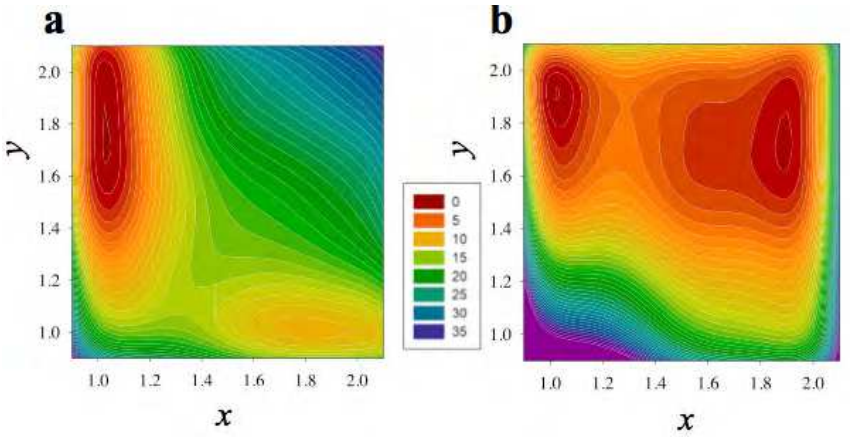

Fig. 6. The potential energy surface of two protons in (a) normal GC pair (b) platinum complex bound GC pair. The unit of the number is kcal/mol.

	j=0	*j*=1	*j*=2	*j*=3	*j*=4	*j*=5	*j*=6
i=0	6935.30	-20913.1	38457.0	-35870.0	18315.3	-4867.65	527.568
i=1	-6004.82	-9088.74	8023.79	-4442.78	1219.89	-131.039	-
i=2	14320.4	4568.72	-1246.22	394.393	-52.4822	-	-
i=3	-14376.9	-2318.65	161.588	-17.1170	-	-	-
i=4	7795.29	692.153	-12.5530	-	-	-	-
i=5	-2195.60	-85.3225	-	-	-	-	-
i=6	251.950	-	-	-	-	-	-

Table 2. Expansion coefficients of C_{ij} in platinum complex bound GC pair.

in normal GC pair, is 15.2 kcal/mol, which gives the similar result to Florian's work [5]. On the other hand, there is no DPT structure of the cisplatin bound GC pair. Figure 7 sketches the optimized structures of the GC and G·C$^+$ pairs, and the transition state (TS). It is confirmed that all of the structures keep their planarity, even after the Pt complex binding and proton transfer. Nevertheless, the distances between the atoms involved in hydrogen bond vary significantly as shown in Table 3. The hydrogen bond of O_6–N_4 increases by 0.15 Å due to the influence of the "additional" hydrogen bond between O_6 and the ligand of cisplatin. The other hydrogen bonds shrink because of the electrostatic interaction induced by the Pt binding, as discussed below. In particular, the hydrogen bond between N_2 (G) and O_2 (C) decreases by 0.19 Å. There is a weak dependence of the ligands in these distances of hydorgen bonds for the GC pair. On the other hand, a stronger dependence is found for the distance between bases of G·C$^+$ pair. O_6–N_4, N_1–N_3, and N_2–O_2 distances in G·C$^+$ pair are shortened by 0.05, 0.08, and 0.02 Å compared with the normal GC pair, respectively. These facts indicate that all of the hydrogen bonds become stronger in comparison with the normal GC pair. In what follows, we examine where these differences arise.

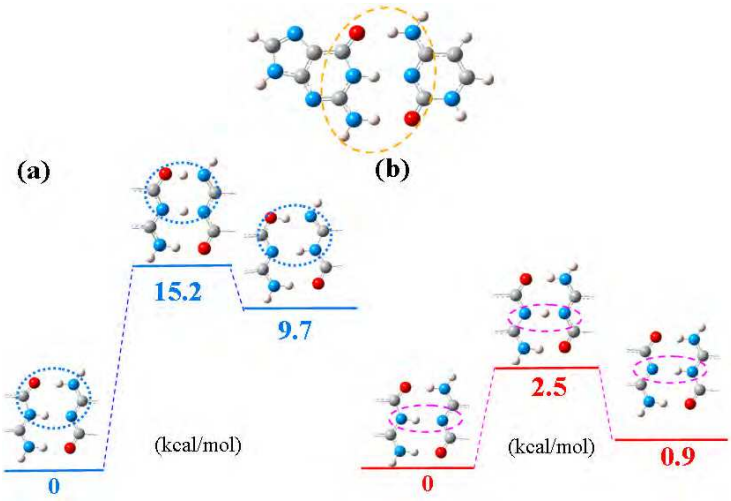

Fig. 7. The reaction diagram for proton-transfer reaction in GC pair. (a) normal GC pair (b) platinum complex bound GC pair. In (a), double proton-transfer reaction occurred, and in (b), single proton-transfer reaction occurred.

	Pt + GC	TS	Pt + G-C$^+$	Experimental
O_6-N_4	3.06	2.80	2.77	2.79
N_1-N_3	2.91	2.64	2.88	2.88
N_2-O_2	2.72	2.77	2.94	2.84

Table 3. Hydrogen bonding length in Pt+GC pairs (in Å)

Charge distributions: The natural bond orbital (NBO) charges of atoms associated with hydrogen bonds and Pt-G coordination, listed in Table 4, shows that in the GC pair the charge on O_6 of G increases by interaction with the ligand of Pt. The hydrogen bond strength between a ligand and O_6 of G influence the charge of O_6, which leads to the difference in the whole hydrogen bonds. The NBO charge on Pt decreases. Therefore, a charge transfer takes place mainly from the guanine and partially from the cytosine to the Pt atom. Such a charge transfer leads to a decrease in the charge on N_1 in guanine and an increase in the charges on all H atoms between the bases. The foregoing discussion gives clues for the reasons why the hydrogen bonds are strengthened: (i) the charge transfer mainly from O_6 of G to the Pt and H atoms, and (ii) additional formation of a hydrogen bond between L_1 and O_6 of G, as pointed out above. Strong dependences of the ligand on the charge of Pt, N_7, and O_6 are found. In the platinum bound GC pair, only a small influence is observed in the Mulliken charges on the atoms in C, whereas the changes are more significant in the G-C$^+$ pair. The charges on all the heavy elements except for O_6 increase compaired to the GC pair. Moreover, strong influences of the ligand on the charge are found for Pt, N_7, O_6, as well as N_1. For further understanding of the interactions among the Pt atom, ligands, and the bases, the sum of the NBO charge on the bases and the ligands are listed in Table 5. As a reference, the total charges in the unbound case is estimated

	Pt-G coordination		Hydrogen bond 1			Hydrogen bond 2			Hydrogen bond 3		
Atom	Pt	N_7	O_6	H_1	N_4	N_1	H_2	N_3	N_2	H_3	O_2
GC	0.72[a]	-0.44	-0.57	0.48	-0.86	-0.81	0.47	-0.64	-0.90	0.46	-0.56
Pt+GC	0.47	-0.63	-0.60	0.46	-0.89	-0.80	0.50	-0.67	-0.87	0.50	-0.57
Pt+G-C$^+$	0.74	-0.53	-0.61	0.47	-0.70	-0.38	0.51	-0.54	-0.69	0.45	-0.32

a: Estimated from $[Pt(NH_3)_4]^{2+}$ as a reference.

Table 4. NBO charges calculated by MP2/LanL2DZ

	G	C	Ligands	Pt
GC pair	-0.026	0.026	1.389	0.611
$Pt(NH_3)_3GC$	0.273	0.125	0.910	0.692
$Pt(NH_3)_3G\text{-}C^+$	-0.444	0.886	0.881	0.686

Table 5. Sum of NBO charge

using $[Pt(NH_3)_4]^{2+}$. In the normal GC pair, both G and C are almost neutral. In contrast, both G and C in the platinum bound GC pair are positive due to the charge transfer from the bases mainly to the Pt atom. As for the G-C$^+$ pair, however, G and C become negative and positive, respectively. Note here that C includes the hydrogen atom that initially belongs to the G in the GC pair as a result of SPT from G to C. Since the charge on the Pt atom increases, charge transfer from G to the ligands of cisplatin accompanies the SPT reaction.

3.5 Summary of section 3

We have numerically elucidated the changes in the hydrogen bonds of the base pairs due to Pt complex formation by means of MP2 theory. For the platinum bound GC pair, the hydrogen bonding energy exceeds by 3–10 kcal/mol than GC pair without platinum complex. The hydrogen bond between O_6–N_4 is lengthened, whereas the other hydrogen bonds are shortened. These observations are explained by a rearrangement of the charge distribution. In this section, we revealed that the binding of platinum complex causes a single proton-transfer (SPT) reaction between N_1 (G) and N_3 (C) in the GC pair. Note here that the SPT reaction does not occur in the GC pair itself, while double proton-transfer (DPT) does. Its reaction barrier decreases from 15-20 kcal/mol of the DPT reaction without the Pt complex to 1.5–3 kcal/mol of the SPT reaction with the Pt complex. The structure that underwent the SPT reaction is as stable as the original structure.

4. Global and local change of GC pairs by coordination of platinum complex

In stacked two GC pairs, althogh DPT reactions can occur independently. However, these reactions hardly take place because of high energy barriers as seen in one GC pair [20]. For further research, it is natural to study what happens when two or more base pairs are stacked. For the simplicity, we hereafter denote a "G-C$^+$ pair" (the product of SPT reaction in GC pair) as a "G*C pair".

4.1 Computational details

Modeling: We first define two types of model systems: the "two base pair" (2bps) model and the "four base pair" (4bps) model. The former consists of two base pairs and cisplatin without the backbone molecules, such as sugar and phosphate groups, while the latter consists of four base pairs and the backbone molecules so that it includes the effects of both the backbone molecules and base stacking.

The 2bps model is small enough to compute with the full quantum chemistry calculation. Density functional theory (DFT) was adopted and the modified Parr–Wang functional (mPW1PW91) was chosen as an exchange–correlation functional, because the functional is modified to better describe the hydrogen bonding. For the calculations described in this chapter, the Stuttgart/Dresden ECPs were used for the Pt atom and the 6-31G (d, p) basis for the other atoms.

ONIOM method: To investigate the effects of DNA stacking, the backbone and counter cations, we proceeded to the 4bps model by ONIOM method introduced in Section 2.3. We here treated two of the four base pairs as the higher layer and the rest as the lower layer. We utilized the method used in the 2bps model for the higher level calculation and the universal force fields (UFF) for the lower level calculation in ONIOM cacluation. We took the initial structure 1,2-d (CpX_1pX_2pT) from PDB (PDBID:1A84), where X_1 and X_2 are purine moieties bound to the Pt complex so that there are three patterns of X_1 and X_2. The ligands of the cisplatin were assumed as NH_3, as in the human body. We also assumed that the Pt atom binds to N_7 of G and A. To keep the whole system neutral, we added sodium atom at every PO_4^- molecule as the counter cation.

4.2 2bps model

Figure 8 shows the all optimized geometries of the three types of model molecules: cis-(CG)-Pt-(GC), cis-(CG)-Pt-(AT) and cis-(TA)-Pt-(AT). The structure of cis-(CG)-Pt-(GC) was distorted in comparison with those in the DNA because of repulsion between the two O_6 atoms. Although one of the GC pairs keeps a planar structure, the other GC pair was greatly distorted. We distinguish them by referring to the former planar pair as the "$(GC)_p$ pair" and the latter distored pair as the "$(GC)_d$ pair". This distortion may lead to the stabiity of whole system in cis-(CG)-Pt-(GC). Hereafter, we will describe the structure of the 2bps model in the form cis-$(GC)_p$-Pt-$(GC)_d$. Unlike the structures of cis-$(GC)_p$-Pt-$(GC)_d$, all base pairs in the cis-(CG)-Pt-(AT) and cis-(TA)-Pt-(AT) almost keep their planarity.

We evaluated the binding energy of cisplatin and the base pair. To estimate the hydrogen bonding energy, we assumed a two-step reaction: (1) $[Pt\ (NH_3)_4]^{2+} + B_p\text{-}B'_p$ -> $[Pt\ (NH_3)_3\ B_p\ B'_p]^{2+} + NH_3$ (reaction energy: ΔE_1) (2) $[Pt\ (NH_3)_3\ B_p\ B'_p]^{2+} + B_d\ B'_d$ -> $[cis\text{-}Pt\ (NH_3)_2\ B_p\ B'_p\ B_d\ B'_d]^{2+} + NH_3$ (reaction energy: ΔE_2), where B_x is A or G, B'_x represents the complementary base of B_x (x = p, d). Results are shown in Table 6. Comparing the ΔE_1 values, the binding energy of Pt-(GC) is much higher than that of Pt-(AT), by 30 kcal/mol. ΔE_1 is larger than ΔE_2 because of the Coulomb repulsion between the original $[Pt\ (NH_3)_3\ B_p\ B'_p]^{2+}$ and the additional base pair. Moreover the bases are likely to bind to the Pt complex in the order cis-(CG)-Pt-(GC), cis-(CG)-Pt-(AT) and cis-(TA)-Pt-(AT). In particular, the binding energy of the cis-(TA)-Pt-(AT) is remarkably low compared with those of cis-(CG)-Pt-(GC) and cis-(CG)-Pt-(AT). These results support both experimental evidence and the tendencies of the models studied by Burda and Leszyczynski [13], as mentioned in the introduction.

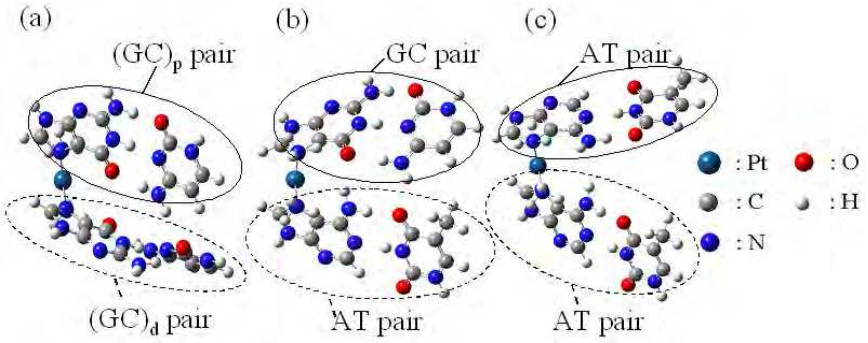

Fig. 8. The optimized structures of the 2bps models: (a) cis-$(CG)_p$-Pt-$(GC)_d$, (b) cis-(CG)-Pt-(AT), and (c) cis-(TA)-Pt-(AT).

	B_1=G, B_2=G	B_1=G, B_2=A	B_1=A, B_2=G	B_1=A, B_2=A
ΔE_1	46.1 (47.9)	46.1 (47.9)	14.7 (16.4)	14.7 (16.4)
ΔE_2	24.5 (25.9)	6.9 (8.2)	38.2 (41.7)	2.4 (4.9)
Total	70.5 (73.8)	52.9 (56.1)	52.9 (56.1)	17.1 (21.3)

a: The "2bps model" was used.
b: The optimized NH_3 and $[Pt(NH_3)_4]^{2+}$ is used for energy calculation.
c: The numbers in parentheses represent the energy including zero-point energy.

Table 6. Energy differences of substitution reaction (in kcal/mol)

Why cisplatin prefers guanine to adenine: Figure 9 shows the reason why cisplatin prefers guanine to adenine. It is known that cisplatin attacks to major groove of DNA base. Guanine has N_7 and O_6 which attract positive charge. On the other hand, adenine has amino group in N_6. One of H atoms in amino group prevent positive charge from attacking to major groove. If cisplatin binds to adenine, this amino group has to be rotated which needs much energy. Thus, cisplatin prefers guanine to adenine. Table 6 shows this tendency exactly. Therefore, we will focus on the models of cis-$(CG)_p$-Pt-$(GC)_d$ and cis-(CG)-Pt-(AT) in further discussion.

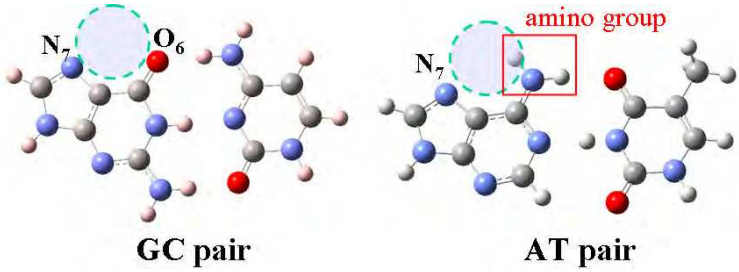

Fig. 9. The major groove of GC and AT pair where cisplatin attacks. In the case of AT pair, amino group of N_6(A) prevents cisplatin from attacking to N_7.

Proton-transfer reactions in 2bps model: Next, we discuss the possibility of multiple proton-transfer reactions in these systems. Here we depict a restricted two-dimensional potential energy surface (PES) of two different hydrogen atoms between N_1 ($G_{p/d}$) and N_3 ($C_{p/d}$) in figure 10, where the geometry except for the two hydrogen atoms is fixed. The rigid PES used here is very rough approximation, because it does not consider the effect of structure relaxation. Nevertheless, it is at least useful to intuitively understand the proton transfer reactions between bases. In this subsection, we depicted this PES in order to confirm whether proton-transferred structures exist or not two stacked base pairs. The origin of the PESs are at the center of both hydrogen bonds, and the PESs were plotted every 0.05 Å. From this figure, it shown that there are three possible minima, at the points marked as X in the figures. No two simultaneous SPT reactions are found because the potential energy of cis-$(CG^*)_p$-Pt-$(G^*C)_d$ is very high as shown in ▲. We here confirmed that one SPT reaction can occur even in two GC pairs. Figure 11 shows the results of geometry optimization of cis-$(CG)_p$-Pt-$(GC)_d$, cis-$(CG^*)_p$-Pt-$(GC)_d$ and cis-$(CG)_p$-Pt-$(G^*C)_d$, where G* again means the guanine donating a proton. This result is similar to the SPT reaction in one GC pair calculation described in previous subsections, where the reaction barrier is about 5–6 kcal/mol. The difference of the energy barrier between cis-$(CG^*)_p$-Pt-$(GC)_d$ and cis-$(CG)_p$-Pt-$(G^*C)_d$ is because of the difference in their planarity. A structure of two simultaneous SPT, cis- $(CG^*)_p$-Pt-$(G^*C)_d$, cannot be found, as expected from the potential surface depicted in figure 10.

Next, the sum of charges obtained by the natural bonding orbital (NBO) is analyzed. Table 7 lists the results of the sum of the NBO charges. Every part of cis-$(CG)_p$-Pt-$(GC)_d$ has a positive charge, but both C_p and C_d are almost neutral. When the SPT reaction occurs, the

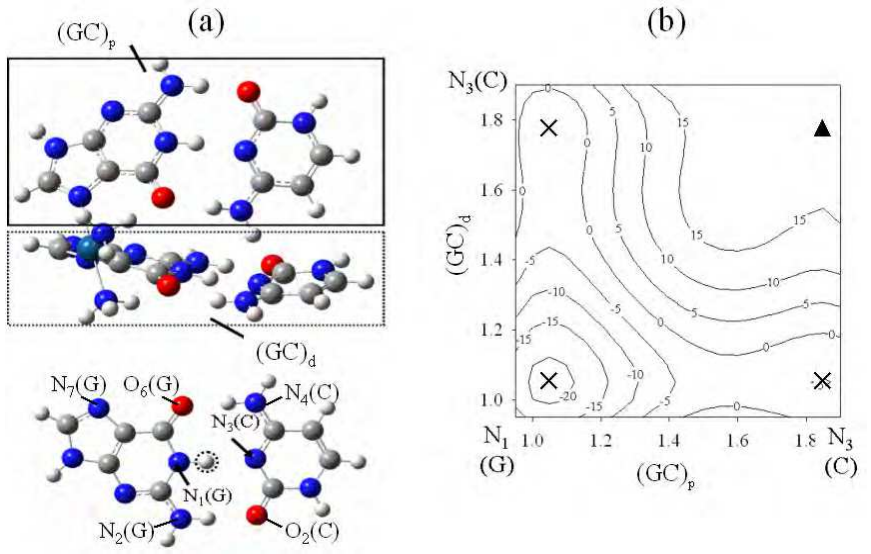

Fig. 10. (a) Definitions of variables in a 2bps model of cis-$(CG)_p$-Pt-$(GC)_d$. Only the hydrogen atoms surrounded by the dotted line in each GC pair were moved. (b) The potential energy surface of hydrogen atoms. The numbers on each axis represent the distance between N_1 (G) and the hydrogen atom (in Å). The origin is set at the point where both hydrogen atoms are at the middle of the hydrogen bonding.

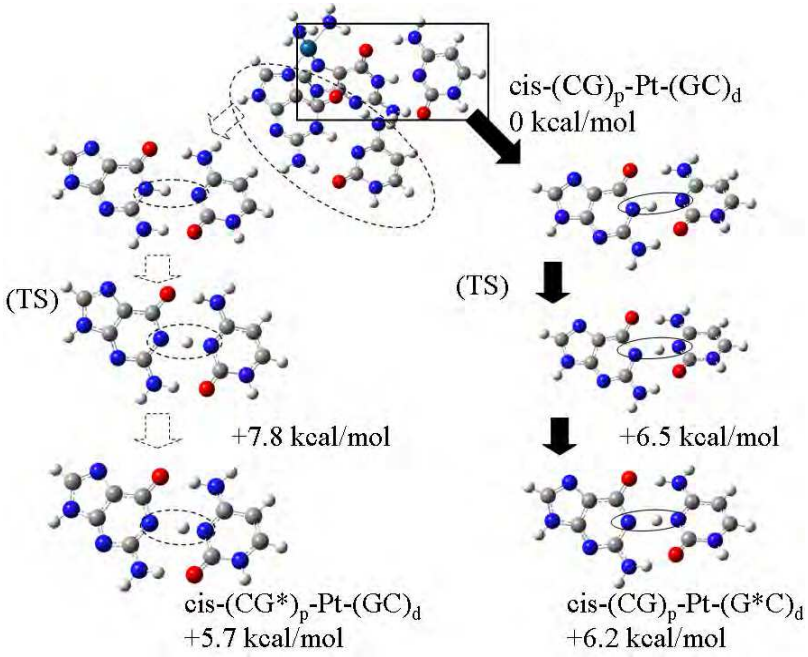

Fig. 11. The reaction diagram for single proton transfer (SPT) between N_1 (G) and N_3 (C) of the 2bps model of cis-(CG)-Pt-(GC). The numbers in kcal/mol in the figure denote relative energies measured from cis-$(CG)_p$-Pt-$(GC)_d$.

	cis-$(CG)_p$-Pt-$(GC)_d$	cis-$(CG^*)_p$-Pt-$(GC)_d$	cis-$(CG)_p$-Pt-$(G^*C)_d$
G_p or G^*_p	0.26	–0.43 [a]	0.25
G_d or G^*_d	0.24	0.25	–0.44 [a]
C_p	0.10	0.58 [b]	0.33
C_d	0.10	0.32	0.58 [b]
Pt	0.73	0.69	0.70
Ligands	0.59	0.58	0.58

a: The sum does not contain the H atom transferred to the N_3 of C.
b: The sum contains the H atom transferred from G.

Table 7. Sum of the charges by natural bond orbital (NBO) analysis

whole charge of a proton donor G* becomes negative. On the other hand, both C_p and C_d become positive after the SPT reaction. The proton donor G* is negative whereas a proton acceptor C is positive. It is expected that these Coulomb repulsions of C_p and C_d and of G_p and G_d prevent further SPT reactions from cis-$(CG)_p$-Pt-$(G^*C)_d$ and $(CG^*)_p$-Pt-$(GC)_d$. In particular, this change of charge distribution can be seen in the case of trans-$(CG)_1$-Pt-$(GC)_2$, in which the two guanines become negative while the two cytosines become positive.

The SPT reaction between N_1 and N_3 of the GC pair also occurs in cis-(CG)-Pt-(AT). The result is similar to the one GC pair shown in Section 3.4. The structure is not distorted in

spite of the SPT reaction between the GC pair. Then, we must know the possibilities of further proton transfers in the AT pair. These pairs have two hydrogen bonds N_6 (A)-O_4 (T) and N_1 (A)-N_3 (T). We show a restricted two-dimensional potential energy surface in Figure 12, where variables r_1 and r_2 denote the distances N_6-H and N_1-H, and the other geometries are fixed. Figure 12 shows two local minima, both cis-(CG)-Pt-(AT) and cis-(CG*)-Pt-(AT). This implies that a multiple SPT reactions can occur in cis-(CG)-Pt-(AT). Nevertheless, the energy difference between local minima is so large that the proton-transfer reaction may not occur at room temperature. The tendency does not change even after the SPT reaction took place in the GC pair. Table 8 summarizes the possibilities for multiple proton-transfer reactions in all the systems.

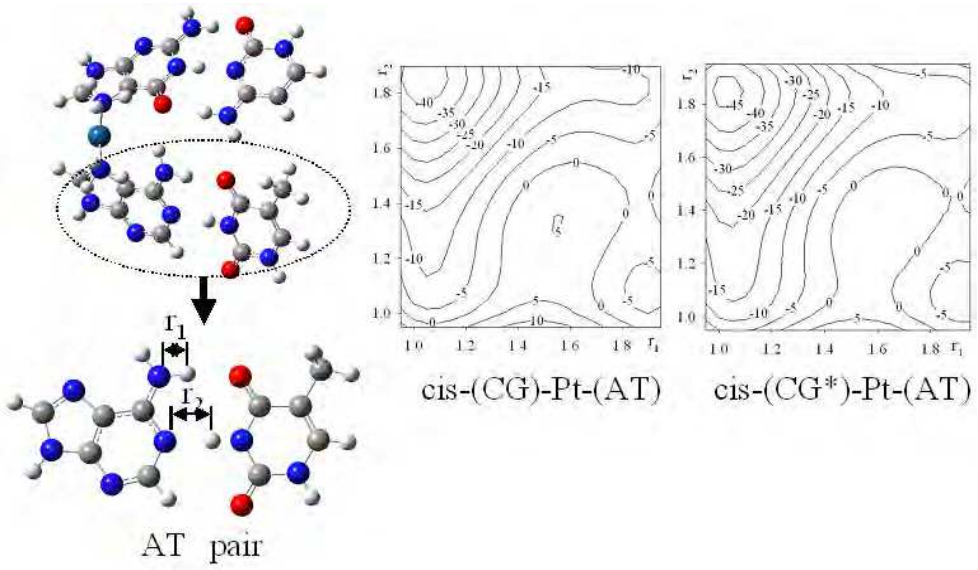

Fig. 12. Definitions of variables in the 2bps model of the cis-(CG)-Pt-(AT). The numbers in the contour plots represent the energy in kcal/mol.

	cis-$(CG)_p$-Pt-$(GC)_d$	
$(CG)_p$ / $(GC)_d$	None	SPT between N_1 and N_3
None	0	6.2
SPT between N_1 and N_3	5.7	N/A (not available)
	cis-(CG)-Pt-(AT)	
GC / AT	None	DPT (N_1 and N_3), (N_6 and O_4)
None	0	17.5
SPT between N_1 and N_3	–1.0	15.2

Table 8. The differences of energy in "2bps. model" molecules (in kcal/mol)

Note that the SPT reaction occurs in platinum-bound GC pair, and the DPT reaction occurs in AT pair. The DPT reaction can also be found even after the SPT reaction between N_1 (G) and N_3 (C) has occurred. The SPT reaction in the AT pair cannot occur, because the Pt complex binding increases the distance between N_1 (A) and N_3 (T). In every case of the DPT reactions, the product of DPT reaction becomes more unstable than the original structure.

4.3 4bps models

Our calculations elucidated that SPT structures of the cis-(CG)-Pt-(GC) type can exist even in 4bps models. Two different optimized structures are shown in Figure 13, which shows one planar GC and one distorted GC pair as well as the 2bps model of cis-(CG)-Pt-(GC). We also found that the backbone and stacking bases do not change their postion much from their original geometry during the SPT reaction.

We extracted the higher layer, i.e., the 2bps and Pt complex, from the 4bps model to investigate the energy differences between cis-$(CG)_p$-Pt-$(GC)_d$ and $(CG^*)_p$-Pt-$(GC)_d$ or cis-$(CG)_p$-Pt-$(G^*C)_d$. The energies of these model molecules are assumed to be approximately those of their higher layer. The energetics of $(CG)_p$-Pt-$(GC)_d$ and $(CG^*)_p$-Pt-$(GC)_d$ are

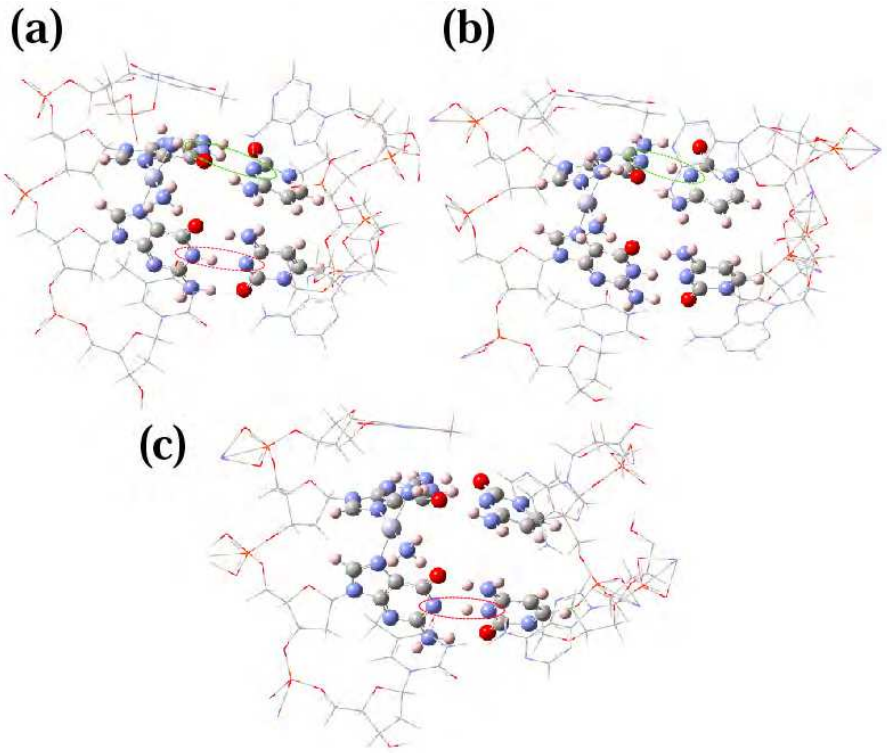

Fig. 13. The optimized structures of the 4bps models of (a) cis-$(CG)_p$-Pt-$(GC)_d$, (b) cis-$(CG^*)_p$-Pt-$(GC)_d$, and (c) cis-$(CG)_p$-Pt-$(G^*C)_d$. Atoms depicted with balls are set to higher layer and with wires are set to lower layer in ONIOM calculations.

shown in Table 9. From this table, the energy differences between the original structure and the proton-transferred structures are estimated as 3-3.5 kcal/mol. From these results, the reaction energy of the SPT reaction is estimated to be lower than the case of 2bps model.

cis-$(CG)_p$-Pt-$(GC)_d$	0
cis-$(CG^*)_p$-Pt-$(GC)_d$	+ 3.2
cis-$(CG)_p$-Pt-$(G^*C)_d$	+ 3.0

a: We set the energy of cis-$(CG)_p$-$(GC)_d$ without sodium atoms as 0.

Table 9. The differences of energy in "4bps model" molecules (in kcal/mol)

We next compared the optimized structure with experimental data from the protein data bank (PDBID: 1A84, 1AU5 and 1KSB) as summarized in Table 10. The hydrogen bond lengths of 1A84 and the optimized structure show poor agreement with each other, where the distance between $(O_6)_d$ and $(N_4)_d$ is about 3.3 Å in the former, which is too large to form hydrogen bonds. Except for this result, the optimized 4bps model of cis-$(CG)_p$-Pt-$(GC)_d$ agrees well with the experimental data in the coordination Pt-G and the error is within 0.05 Å. On the other hand, the error of the hydrogen bond length is significant, e.g., the hydrogen bond length of $(O_2)_p$-$(N_2)_p$ is 2.75 Å for the 4bps model of cis-$(CG)_p$-Pt-$(GC)_d$ and 2.96 Å for 1AU5. This is because the energies of cis-$(CG^*)_p$-Pt-$(GC)_d$ and cis-$(CG)_p$-Pt-$(G^*C)_d$ are as stable as those of cis-$(CG)_p$-Pt-$(GC)_d$ so that the mean of these structures may be observed in the experiment because of the low energy barrier of the SPT reaction. Indeed, the error is improved when the structures of cis-$(CG^*)_p$-Pt-$(GC)_d$ and cis-$(CG)_p$-Pt-$(G^*C)_d$ are taken into account. In this case, it is possible that the dynamic fluctuations may dominate the structure of the system.

	cis-$(CG)_p$-Pt-$(GC)_d$	cis-$(CG^*)_p$-Pt-$(GC)_d$	cis-$(CG)_p$-Pt-$(G^*C)_d$	1A84	1AU5	1KSB
Pt-G coordination						
[a]Pt-G_p	2.04	2.03	2.04	2.05	1.96	2.01
[a]Pt-G_d	2.04	2.04	2.03	2.05	1.98	2.01
[b]Gp-Pt-Gd	89.4	91.4	89.6	90.1	87.4	88.6
G_p-Pt-L_1-G_d	53.7	58.6	63.3	40.8	–1.4	56.9
G_p-Pt-L_2-G_d	69.2	69.5	64.6	72.9	–17.5	55.3
Hydrogen bond length						
$(O_6)_p$-$(N_4)_p$	2.84	2.62	2.85	2.97	2.73	2.76
$(N_1)_p$-$(N_3)_p$	2.85	2.77	2.87	3.01	2.96	2.86
$(O_2)_p$-$(N_2)_p$	2.73	2.92	2.79	2.91	2.87	2.91
$(O_6)_d$-$(N_4)_d$	2.82	2.92	2.65	3.28	2.80	2.83
$(N_1)_d$-$(N_3)_d$	2.81	2.84	2.76	2.99	2.71	2.89
$(O_2)_d$-$(N_2)_d$	2.75	2.74	2.96	2.59	2.96	2.85

a: The distance Pt-G is defined as the distance between Pt and N_7 of guanine.
b: The angle G_p-Pt-G_d is defined as N_7 (G_p)-Pt-N_7 (G_d).
c: The unit of distance is angstrom, the unit of angle is degree.

Table 10. Selected lengths of optimized geometries and the experimental data from the protein databank

For further research, it is also necessary to discuss the possibilities of proton-transfer in larger system. In such systems, it is necessary to consider not only the optimized structure but also structural fluctuations. The mean structure between the original and the SPT structures may be observed at room temperature. The dynamic effects will be investigated in our future work.

4.4 Summary of section 4

The binding affinity of cisplatin to base pairs were in the following order in our calculation, cis-(CG)-Pt-(GC), cis-(CG)-Pt-(AT), and cis-(TA)-Pt-(AT), when complementary base pairs were taken into account. From their energetics, the structure of cis(TA)-Pt-(AT) is expected to be notfound at room temperature. The SPT reaction can occur in systems that consist of two base pairs and cisplatin. The reaction barrier is as low as 6–7 kcal/mol, which is similar to the case of one GC pair with cisplatin, and the SPT structure is as stable as the original structure. From these results, it is possible that the coordination of cisplatin to DNA causes a mispairing of the GC pair that leads to a mutation of the DNA. The SPT reaction causes this in one of the GC pairs. On the other hand, two simultaneous SPT structures like cis-(CG*)-Pt-(G*C) are forbidden. This is explained by the analysis of charge distributions. After one SPT reaction occurs, the proton donor G becomes negative and the proton acceptor C positive. At the same time, the other C also becomes positive through electrostatic effect from virtically stacked base pair that under went SPT reaction. Therefore, the subsequent SPT reaction from the other G is forbidden by Coulomb repulsion. The SPT reaction between G and C can occur with cis-(CG)-Pt-(AT). This result is similar to the case of one GC pair.

By using the ONIOM method, the SPT reaction is also shown to occur in the system consisting of cisplatin and four base pairs containing the backbone molecules (4bps model). Without the effects of the backbone and the stacking base pairs, the structure of cis-$(CG)_p$-Pt-$(GC)_d$ is so distorted that we cannot expect it to describe the actual structure in the DNA. The optimized structure of the 4bps cis-(CG)-Pt-(GC) model agrees with results from NMR experiments in view of the Pt-G coordination, but not of the hydrogen bond length. Because the structures of cis-$(CG^*)_p$-Pt-$(GC)_d$ and cis-$(CG)_p$-Pt-$(G^*C)_d$ are as stable as the original one, their mean structures may be observed in experiments.

5. Conclusion

We investigated the change of proton-transfer reactions in DNA base pairs caused by the coordination of cisplatin by density functional theory (DFT) and ONIOM method. When the cisplatin binds to GC pair, the structure undergoes intermolecular proton transfer from G to C (denoted as G*C pair) resulting in an increase of the bonding energy by 3-10 kcal/mol. This renders the structure to be metastable due to (a) successive processes of charge transfer from G to cisplatin thereby stabilizing the GC and G*C pairs and (b) an additional hydrogen bond between G and the ligand of Pt atom. From the energetics of two base pairs with the cisplatin, it is theoretically confirmed that the Pt complex is likely to bind in the following order: cis-(CG)-Pt-(GC), cis-(CG)-Pt-(AT), cis-(TA)-Pt-(AT).The Pt atom is expected to bind to the N_7 site of G and A. This result supports the experimental evidence, where the structure cis-A-Pt-A is seldom observed at room temperature. The single proton-transfer reaction occurs in one of the two GC pairs. No simultaneous single proton-transfer reaction can occur in both base pairs. Two different single proton-transferred structures (cis-$(CG^*)_d$-

Pt-$(GC)_p$ and cis-$(CG)_d$-Pt-$(G^*C)_p$, where * means a proton donor of G) are as stable as the original structures $(CG)_d$-Pt-$(GC)_p$. The same tendency was observed with cis-(CG*)-Pt-(AT). In contrast to cisplatin, multiple single proton-transfer reactions may occur in the system consisted of two base pairs with transplatin. The optimized structure agrees with the experimental data for Pt-G coordination except for the hydrogen bond length.

6. Acknowledgment

This study is supported by a Grant-in-Aid for Young Scientists (A) (No. 22685003) from Japan Society for the Promotion of the Science (JSPS) T.M. is thankful to the research fellowship for young scientists from JSPS. We thank Prof. S. Sakaki in Kyoto University for helpful advice.

7. References

[1] Jurečka, P. & Hobza, P. (2003). True Stabilization Energies for the Optimal Planar Hydrogen-Bonded and Stacked Structures of Guanine·Cytosine, Adenine·Thymine, and Their 9- and 1-Methyl Derivatives: Complete Basis Set Calculations at the MP2 and CCSD(T) Levels and Comparison with Experiment. *Journal of the American Chemical Society* Vol.125, No.50, (December 17, 2003), pp. 15608-15613, ISSN 0002-7863.

[2] Šponer, J. & Jurečka, P.; Hobza, P. (2004). Accurate Interaction Energies of Hydrogen-Bonded Nucleic Acid Base Pairs. *Journal of the American Chemical Society*, Vol.126, No.32, (August 18, 2004), pp. 10142-10151, ISSN 0002-7863.

[3] Löwdin, P.-O. (1963). Proton Tunneling in DNA and its Biological Implications. *Review of Modern Physics*, Vol.35, No.3, (July-September), pp. 724-732, ISSN 1539-0756.

[4] Florián, J.; Hrouda, V. & Hobza, P. (1994). Proton Transfer in the Adenine-Thymine Base Pair. *Journal of the American Chemical Society*, Vol.116, No.4, (February, 1994), pp.1457-1460, ISSN 0002-7863.

[5] Florián, J. & Leszczynski, J. (1996). Spontaneous DNA Mutations Induced by Proton Transfer in the Guanine·Cytosine Base Pairs: An Energetic Perspective. *Journal of the American Chemical Society*, Vol.118, No.12, (March 27, 1996), pp.3010-3017, ISSN 0002-7863.

[6] Villani, G. (2006). Theoretical investigation of hydrogen transfer mechanism in the guanine-cytosine base pair. *Chemical Physics*, Vol.324, No.2-3, (May 31, 2006), pp. 438-446, ISSN 0301-0104.

[7] Shigeta, Y.; Miyachi, H.; Matsui, T. & Hirao, K. (2008). Dynamic Quantum Isotope Effects on Multiple Proton-Transfer Reactions. *Bulletin of Chemical Society of Japan*, Vol.81, No.10, (October, 2008), pp. 1230-1240, ISSN 1348-0634.

[8] Yamamura, M.; Ichino, T. & Yoshioka, Y. (2011). A B3LYP Study on Repair of Guanyl and 8-Oxoguanyl Radical by Simultaneous Proton- and Electron-Transfer Reaction. *Bulletin of Chemical Society of Japan*, Vol.84, No.2, (February, 2011), pp. 181-190, ISSN 1348-0634.

[9] Matsui, T.; Shigeta, Y. & Hirao, K. (2006). The influence of Pt complex between guanine-cytosine pair, *Chemical Physics Letters*, Vol.423, No.4-6(June 1, 2006), pp.331-334, ISSN 0006-2614.

[10] Matsui, T.; Shigeta, Y. & Hirao, K. (2007). Multiple proton-transfer reactions in guanine-cytosine pairs by the coordination of Pt complex. *The Journal of Physical Chemistry B*, Vol.111, No. 5(February 15), pp.1176-1181, ISSN 1520-6106.

[11] Rosenberg, B.; van Camp, L.; Trosko, J. L. & Mansour, V.H. (1969), Platinum Compounds: a New Class of Potent Antitumour Agents. *Nature*, Vol.222, No.5191, (April 26, 1969), pp. 385-386, ISSN 0028-0836.

[12] Eastman, A. (1986), Reevaluation of interaction of cis-dichloro(ethylenediamine) platinum(II) with DNA. *Biochemistry* Vol. 25, No.13, (July, 1986), pp. 3912-3915, ISSN 0006-2960.

[13] Burda, J.V. & Leszczynski, J. (2003). How strong can the bend be on a DNA helix from cisplatin? DFT and MP2 quantum chemical calculations of cisplatin-bridged DNA purine bases. *Inorganic Chemistry*, Vol.42, No.22, (November 3, 2003), pp.7162-7172, ISSN 0020-1669.

[14] Zeizinger, M.; Burda, J.V. & Leszczynski, J. (2004). The influence of a sugar-phosphate backbone on the cisplatin-bridged BpB' models of DNA purine bases. Quantum chemical calculations of Pt(II) bonding characteristics. *Physical Chemistry Chemical Physics*, Vol.6, No.13 (July 7, 2004), pp.3585- ISSN 1463-9076.

[15] Szabo, A. & Ostlund, N.S. (1996). *Modern Quantum Chemistry: Introduction to Advanced Electronic Structure Theory*, Dover publications, ISBN 978-0486691862, New York, USA.

[16] Jensen, F. (2006). *Introduction to Computational Chemistry 2nd edition,* John Wiley & Sons, ISBN 978-0471984252, Chichester, UK.

[17] Adamo, C. & Barone, V.(1998). Exchange functionals with improved long-range behavior and adiabatic connection methods without adjustable parameters: The mPW and mPW1PW models, *Journal of Chemical Physics*, Vol.108, No.2 (Jan 8, 1998), pp.664-675, ISSN 1089-7690.

[18] Svensson, M.; Humbel, S.; Froese, R.D.J.; Matsubara, T.; Sieber, S. & Morokuma, K. (1996). ONIOM: A multi-layered integrated MO+MM method for geometry optimizations and single point energy predictions. A test for Diels-Alder reactions and $Pt(P(t\text{-}Bu)_3)_2+H_2$ oxidative addition. *The Journal of Physical Chemistry*, Vol.100, No.50(December 13, 1996), pp.19357-19363, ISSN 1520-6106.

[19] Frisch, M.J. et al. (2004). *Gaussian 03*, *Revision C.02*, Gaussian, Inc., Wallingford CT, USA.

[20] Matsui, T.; Sato, T. & Shigeta, Y. (2009). Sequence dependent proton-transfer reaction in stacked GC pair I: The possibilities of proton-transfer reaction. *International Journal of Quantum Chemistry*, Vol.109, No.10(August 15, 2009), pp.2168-2177, ISSN 0020-7608.

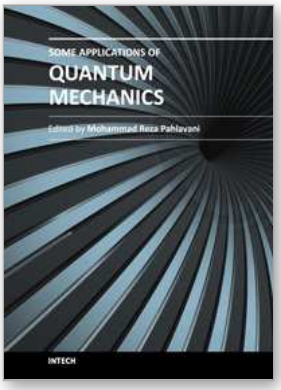

Some Applications of Quantum Mechanics

Edited by Prof. Mohammad Reza Pahlavani

ISBN 978-953-51-0059-1
Hard cover, 424 pages
Publisher InTech
Published online 22, February, 2012
Published in print edition February, 2012

Quantum mechanics, shortly after invention, obtained applications in different area of human knowledge. Perhaps, the most attractive feature of quantum mechanics is its applications in such diverse area as, astrophysics, nuclear physics, atomic and molecular spectroscopy, solid state physics and nanotechnology, crystallography, chemistry, biotechnology, information theory, electronic engineering... This book is the result of an international attempt written by invited authors from over the world to response daily growing needs in this area. We do not believe that this book can cover all area of application of quantum mechanics but wish to be a good reference for graduate students and researchers.

InTech Europe
University Campus STeP Ri
Slavka Krautzeka 83/A
51000 Rijeka, Croatia
Phone: +385 (51) 770 447
Fax: +385 (51) 686 166
www.intechopen.com

InTech China
Unit 405, Office Block, Hotel Equatorial Shanghai
No.65, Yan An Road (West), Shanghai, 200040, China
中国上海市延安西路65号上海国际贵都大饭店办公楼405单元
Phone: +86-21-62489820
Fax: +86-21-62489821